

Accepted Manuscript

Structure and mechanical properties of sodium and calcium caseinate edible active films with carvacrol

Marina P. Arrieta, Mercedes A. Peltzer, María del Carmen Garrigós, Alfonso Jiménez

PII: S0260-8774(12)00428-1

DOI: <http://dx.doi.org/10.1016/j.jfoodeng.2012.09.002>

Reference: JFOE 7079

To appear in: *Journal of Food Engineering*

Received Date: 4 July 2012

Revised Date: 6 September 2012

Accepted Date: 8 September 2012



Please cite this article as: Arrieta, M.P., Peltzer, M.A., Garrigós, a.d.C., Jiménez, A., Structure and mechanical properties of sodium and calcium caseinate edible active films with carvacrol, *Journal of Food Engineering* (2012), doi: <http://dx.doi.org/10.1016/j.jfoodeng.2012.09.002>

This is a PDF file of an unedited manuscript that has been accepted for publication. As a service to our customers we are providing this early version of the manuscript. The manuscript will undergo copyediting, typesetting, and review of the resulting proof before it is published in its final form. Please note that during the production process errors may be discovered which could affect the content, and all legal disclaimers that apply to the journal pertain.

Structure and mechanical properties of sodium and calcium caseinate edible active films with carvacrol

Marina P. Arrieta^{a,b*}, Mercedes A. Peltzer^a, María del Carmen Garrigós^a and Alfonso Jiménez^a

^a Department of Analytical Chemistry, Nutrition and Food Sciences, University of Alicante, P.O. Box 99, E-03080 Alicante, Spain.

^b Department of Mechanical and Materials Engineering, Polytechnic University of Valencia, Plaza Ferrandiz y Carbonell 1, 03801 Alcoy, Alicante Spain.

*Corresponding author. Tel: +34-965903117. Fax: +34-965903697

E-mail address: marina.arrieta@ua.es, marrieta@itm.upv.es (M.P. Arrieta)

Postal address: Carretera San Vicente del Raspeig s/n. P.O. Box 99, E-03080 San Vicente del Raspeig, Alicante, Spain.

Abstract:

Edible active films based on sodium caseinate (SC) and calcium caseinate (CC) plasticized with glycerol (G) at three different concentrations and carvacrol (CRV) as active agent were prepared by solvent casting. Transparent films were obtained and their surfaces were analysed by optical microscopy and scanning electron microscopy (SEM). The influence of the addition of three different plasticizer concentrations was studied by determining tensile properties, while Fourier transformed infrared spectroscopy (FTIR) and thermogravimetric analysis (TGA) were used to evaluate the structural and thermal behaviour of such films. The addition of glycerol resulted in a reduction in the elastic modulus and tensile strength, while some increase in the elongation at break was observed. In general terms, SC films showed flexibility higher than the corresponding CC counterparts. In addition, the presence of carvacrol caused further improvements in ductile properties suggesting the presence of stronger

interactions between the protein matrix and glycerol, as it was also observed in thermal degradation studies. FTIR spectra of all films showed the characteristic bands and peaks corresponding to proteins as well as to primary and secondary alcohols. In summary, the best results regarding mechanical and structural properties for caseinates-based films containing carvacrol were found for the formulations with high glycerol concentrations.

Keywords: edible films; caseinates; glycerol; carvacrol; active packaging.

1. INTRODUCTION

An increasing proactive attitude of society towards a reduction on the environmental impact produced by food packaging after use is currently growing. This could be joined to the consumer's demand for higher quality and longer shelf life food with an increase on research in new active packaging formulations. Under this general framework, the research on biopolymer-based packaging materials is being extensively explored (Juvonen et al., 2011; Verbeek and Van den Berg, 2010). Another raising tendency in food packaging research is the study of interactions between materials and foodstuff to take advantage of the controlled migration of active additives. Some of them can be extracted from essential oils obtained from aromatic plants with antimicrobial activities (Chalier et al., 2007; Peltzer et al., 2009). They can be used to control spoilage and pathogens proliferation in food during storage and distribution (Ben Arfa et al., 2007; Moreira et al., 2011; Viuda-Martos et al., 2007). Antimicrobial agents can be added by coating onto the food surface or could be incorporated into food-packaging materials with controlled migration to foodstuff (Kristo et al., 2008).

The coordination of both concepts (i.e. sustainability and active packaging) could result in the development of edible films with antimicrobial properties to be used in food packaging materials (Ponce et al., 2008; Quintavalla and Vicini, 2002). In this sense, carvacrol, a volatile aromatic compound extracted from oregano and thyme

essential oils, is well known for its antimicrobial activity (Lu et al., 2011; Mascheroni et al., 2010; Nostro et al., 2007; Viuda-Martos et al., 2010; Viuda-Martos et al., 2011; Viuda-Martos et al., 2007). Oregano oil has been widely used as a dietary supplement for combating infections and relieving digestive and skin-related problems (Cho et al., 2012).

The use of biopolymers as matrices in active packaging systems has been relatively unexplored despite their sustainability and advantageous properties. For instance, proteins are adequate for the preparation of biofilms by their high plasticity and elasticity (Pereda et al., 2008; Pereda et al., 2011). In addition, they are abundant in Nature and fully renewable (Ponce et al., 2008) since they can be obtained from plants (corn zein, wheat gluten, soy or sunflower) and animal sources (gelatin, keratin, casein or whey) (Hernandez-Izquierdo and Krochta, 2008; Verbeek and Van den Berg, 2010). Among them, caseinates can be considered attractive for their use in food packaging, since they show numerous functional properties, such as water solubility and ability to act as emulsifiers (Fabra et al., 2009; Jimenez et al., 2012; Pereda et al., 2010). In addition, due to the high number of polar groups in their structure, caseinates also show good adhesion to different substrates making them excellent barrier to non-polar substances, such as oxygen, carbon dioxide and aromas (Audic et al., 2003). However, due to the inherent brittleness of many biopolymers including caseinates, plasticizers should be necessarily used to improve their ductile properties and to get the flexibility required for films manufacturing (Martino et al., 2009). In this sense, the use of glycerol has been proposed, since it contributes to the reduction in material brittleness by the limitation of crosslinking and elimination of intra and intermolecular hydrogen bonds (Pereda et al., 2008)). Furthermore, it should be pointed out that glycerol is a by-product of biodiesel production; so, it would be positive to increase its added value from a low-grade by-product to a useful plasticizer (Ye et al., 2012).

Some studies have been recently performed with casein and caseinates as matrices for edible films. For instance, nano-biocomposites based on casein and

sodium montmorillonites were recently studied (Pojanavaraphan et al., 2010). Other authors used modified sodium caseinate as matrix for edible films containing oleic acid-beeswax mixtures (Fabra et al., 2009) or tung oil (Pereda et al., 2010). Antimicrobial edible films were also obtained from sodium caseinate and chitosan blends (Pereda et al., 2008) or nisin (Cao-Hoang et al., 2010). In this work we compare two commercial caseinates in their use as matrices for polymer edible films. Carvacrol was chosen as antimicrobial agent in these formulations since this compound presents several positive characteristics. It is a natural compound with antimicrobial activity against a broad range of bacteria and it is categorized as GRAS (FDA Administration US). Carvacrol has been recently used as active additive in different formulations for active packaging with promising results (Gutierrez et al., 2010; Persico et al., 2009; Ramos et al., 2012). However, at the best of our knowledge the addition of carvacrol into sodium or calcium caseinates for edible films manufacturing has not been reported.

The aim of the present work is the development of carvacrol edible active films based on sodium and calcium caseinates plasticized with glycerol. Films were obtained by solvent casting and further characterized to evaluate their viability for food packaging applications, regarding their structure, mechanical and thermal properties.

2. EXPERIMENTAL

2.1 Materials

Sodium (SC) and calcium caseinates (CC) were kindly supplied in powder form by Ferrer Alimentación S.A (Barcelona, Spain). Carvacrol (98%) and anhydrous glycerol (99.5%) were purchased from Sigma Aldrich (Móstoles, Madrid, Spain).

2.2 Films preparation

Films were prepared by solvent casting. Solutions were prepared in distilled water with 5 wt% of caseinate, either SC or CC. Glycerol was added to obtain protein:glycerol ratios 1:0, 1:0.15, 1:0.25, 1:0.35. Solutions were then heated at 65 °C

for 10 minutes under continuous stirring at 1100 rpm and further cooled at room temperature. The final pH of these caseinates-glycerol solutions was 6.95. Furthermore, carvacrol was added at 10 wt% resulting in a final protein:carvacrol ratio 1:0.10, with homogenization for 3 min at 1100 rpm. The pH of these solutions was between 5.35 and 5.40. Finally, ultrasonic degasification at room temperature was applied to all solutions to eliminate foams and air bubbles.

Films were prepared by taking 30 mL of these solutions into 15-cm diameter polyethylene Petri dish containers (Distrilab S.L., Cartagena, Spain). They were conditioned at 25 ± 2 °C and 50% constant relative humidity (RH) in a Dycometal-CM81 climatic test chamber (Barcelona, Spain) for 48 h.

The average thickness of films was measured with a Digimatic Micrometer Series 293 MDC-Lite (Mitutoyo, Japan) ± 0.001 mm at ten random positions over the film surface.

2.3. Characterization

Thermogravimetric analysis (TGA) tests were carried out by using a TGA/SDTA 851 Mettler Toledo thermal analyzer (Schwarzenbach, Switzerland). Samples weighing around 5-10 mg were heated from room temperature to 700 °C at $10^\circ \text{C min}^{-1}$ under nitrogen atmosphere (50 mL min^{-1}) and from 700 °C to 900 °C at the same heating rate under oxygen atmosphere (50 mL min^{-1}) with the aim of determining the inorganic residue in each formulation. The initial degradation temperature (T_0) was calculated at 10% mass loss, while temperatures at the maximum degradation rate (T_{max}) for each stage were determined from the peaks of the derivative curves (DTG).

Fourier transformed infrared spectroscopy (FTIR) tests were carried out by using a Perkin-Elmer infrared spectrometer (Perkin Elmer Spain, S.L., Madrid Spain). Samples were cut in 1cm x 1cm squares, with average thicknesses $88 \pm 16 \mu\text{m}$ for SC and $103 \pm 11 \mu\text{m}$ for CC films, and were analysed at room temperature and 50% RH. Attenuated total reflectance (ATR) spectra were obtained in the $4000\text{-}600 \text{ cm}^{-1}$ region,

using 128 scans and 4 cm⁻¹ resolution. A blank spectrum was obtained before each test to compensate the humidity effect and the presence of carbon dioxide in the air by spectra subtraction.

Samples surfaces were observed by an optical microscopy (Olympus BH2-UMA Microscope), with no further preparation, by ordinary light.

Scanning electronic microscopy (SEM) surface and cross section tests were carried out with a JEOL JSM-840 microscope (Jeol USA Inc., Peabody, USA), operated at 10 kV. 10 x 10 mm² samples were cut and coated with gold layer (10-25 nm) prior to analysis in order to increase their electrical conductivity. Images were registered at 1000x magnification.

Tensile tests were carried out at room temperature and 50% RH by using a 3344 Instron Instrument (Fareham Hants, UK) according to ASTM D882-01 Standard (ASTM, 2001). Tests were performed in rectangular strips (10 x 100 mm²), initial grip separation 50 mm and crosshead speed 25 mm min⁻¹. Average percentage deformation at break (ϵ_B %), elastic modulus (E) and tensile strength (TS) were calculated from the resulting stress-strain curves as the average of five measurements from three films of each composition.

3. RESULTS AND DISCUSSION

Transparent SC and CC edible films were successfully obtained by following the above-described procedure. No apparent differences in transparency and colour can be reported for samples containing carvacrol after comparison with the non-active counterparts (Figure 1). However, samples containing carvacrol showed a slightly characteristic oregano odor. Average thicknesses were 88 ± 16 µm for SC and 103 ± 11 µm for CC films.

3.1 Thermal properties

Table 1 and 2 summarize the TGA results for the SC and CC edible films, respectively. Pure SC and CC showed similar degradation patterns, with two main thermal events. The first one was observed around 120-140 °C corresponding to the evaporation of absorbed and bound water in caseinates structure. The second stage was associated to their degradation and it was observed from 189 °C (T_0) for SC and 198 °C (T_0) for CC, reaching T_{max} at 330 °C and 338 °C, respectively. The residue at 700 °C was around 25% in both cases.

Pure glycerol showed a single degradation step, with T_0 146 °C and T_{max} 269 °C. No residue at 700 °C was observed. On the other hand, carvacrol degraded in two steps, with T_{max} at 92 °C and 208 °C. The residual waste after degradation at 700 °C was negligible.

In general terms, TGA curves for films showed more than one degradation step. Non-plasticized films (i.e. pure SC and CC) showed the same TGA pattern than the original powder. Nevertheless, it should be noted that caseinate/glycerol blends showed lower decomposition temperatures than non-plasticized films, indicating a decrease in thermal stability caused by the presence of plasticizer. This result can be explained by the influence of glycerol on the reduction in the number of inter and intramolecular bonds in the protein structure, resulting in a decrease of thermal stability of the whole system (Barreto et al., 2003).

On the other hand, plasticized films with carvacrol showed three degradation steps (Figure 2). The first event was observed at temperatures around 100 °C and it was related to the loss of moisture and bound water remaining from the casting process. The second stage at temperatures between 200 °C and 250 °C could be related to the loss of glycerol and carvacrol from the material. A similar behaviour was described by other authors indicating that glycerol can be easily eliminated from caseinate films at temperatures between 105-239 °C (Pereda et al., 2008). Finally, the third degradation process, at temperatures above 300 °C, was associated to the protein thermal degradation. This sequential degradation of these films during heating

could be explained by the gradual loss of the initial ordered structure of the polymer matrix, since inter and intra-molecular hydrogen bonding are broken up at raising temperatures (Barreto et al., 2003). As it has been reported, the presence of additives in these formulations contributes to the decrease in the number of protein-protein bonds, resulting in lower thermal stability of these samples (Verbeek and Van den Berg, 2010). In general CC films showed higher thermal stability than those based on SC. This result could be explained by considering that divalent calcium cations in CC promote cross-linking with protein chains, giving rise to a more rigid structure with higher thermal stability (Fabra et al., 2010).

However, in CC films the presence of carvacrol had no influence on protein-protein bonds since the maximum degradation temperature remained nearly constant for all films. As expected, it was observed that the T_0 decreased with the addition of higher amounts of glycerol in SC and CC films indicating a good incorporation of the plasticizer to the polymer matrix.

3.2 FTIR analysis

3.2.1 Raw materials

Molecular interactions in blends were studied by obtaining their FTIR spectra. The analysis of films obtained from raw materials was performed and results for glycerol and carvacrol as well as for SC and CC in powder form are shown in Figure 3. The spectrum for glycerol (Figure 3a) shows the typical bands for alcohols, with the stretching absorption associated with the hydroxyl groups (-OH) in the $3600\text{-}3000\text{ cm}^{-1}$ range, while the carbon-oxygen (C-O) absorption peaks characteristic of primary and secondary alcohols were observed at 1030 and 1100 cm^{-1} , respectively. In addition, peaks for CH-OH bending were observed at $1125\text{-}1100\text{ cm}^{-1}$, while $\text{CH}_2\text{-OH}$ bending bands appeared at $1075\text{-}1000\text{ cm}^{-1}$. Bands in the $1400\text{-}1200\text{ cm}^{-1}$ range can be assigned to the in-plane bending of the hydroxyl group. Finally, asymmetric and

symmetric stretching vibrations associated with carbon-hydrogen (C-H) bonds were identified at 2875 cm^{-1} and 2925 cm^{-1} , respectively (Pretsch, 2001).

The spectrum for carvacrol (Figure 3b) also showed wide stretching absorption bands associated to the -OH stretching region from 3650 to 3100 cm^{-1} . Peaks observed between 1600 and 1400 cm^{-1} could be attributed to the aromatic ring insaturations in the carvacrol molecule, particularly to in-ring carbon-carbon stretching. Stretching vibration peaks for the aromatic hydroxyl groups were identified around 1250 cm^{-1} . Out of plane stretching peaks due to aromatic C-H bonds were observed in the $900\text{-}650\text{ cm}^{-1}$ range. Asymmetric and symmetric stretching vibrations of C-H bonds (2867 cm^{-1}), symmetric stretching of -CH_3 (1380 cm^{-1}) and bending of -CH_3 (1340 cm^{-1}) were also assigned. Finally, the aromatic C=C stretching was identified at 800 cm^{-1} . Overtones characteristic of aromatic compounds were present as weak bands in the $2000\text{-}1665\text{ cm}^{-1}$ region (Pretsch, 2001).

The spectra for caseinates (Figure 3e) showed strong amide I and amide II peaks between $1700\text{-}1500\text{ cm}^{-1}$ and the -NH group stretching at $3400\text{-}3000\text{ cm}^{-1}$ characteristic of amino acids, as it was previously reported by other authors (Oliver et al., 2009; Pereda et al., 2008). A small shoulder at 3080 cm^{-1} could be assigned to the primary amines structure, being probably an overtone of the amide II absorption peak (Pereda et al., 2008). Peaks at 1630 cm^{-1} in the amide I region and 1510 cm^{-1} in the amide II region could be assigned to the stretching of the carbonyl group (C=O) and to the symmetric stretching of N-C=O bonds, respectively. The bands around 1400 cm^{-1} could be assigned to the carboxylate group (O-C-O) (Abu Diak et al., 2007). The bands at 1174 cm^{-1} and 1066 cm^{-1} for SC and at 1160 cm^{-1} and 1091 cm^{-1} for CC resulted from the C-O stretching in C-OH bonds (Pelissari et al., 2009). The most important differences between the spectra for SC and CC in powder were found at low wavenumbers (Figures 3e). In agreement with results reported by other authors (Pelissari et al., 2009; Wang et al., 2007), SC had the C-O stretching band in C-OH at 1076 cm^{-1} , while CC showed these bands at 1090 and 1156 cm^{-1} . It was reported that

monoanionic phosphates showed symmetric stretching bands around 1080 cm^{-1} while the same band appeared at 976 cm^{-1} in dianionic phosphates (Fernandez et al., 2003). In this study, SC showed a band at 974 cm^{-1} and CC at 995 cm^{-1} suggesting monocationic and dicationic interactions with Na^+ and Ca^{+2} , respectively.

3.2.2 SC, CC, SC/G/CRV and CC/G/CRV edible films

FTIR spectra corresponding to the SC powder, G and SC films with different glycerol concentrations in the $3600\text{--}2800\text{ cm}^{-1}$ range (corresponding to --OH and --NH stretching bands) are shown in Figure 4a. Due to the caseinates random coil nature and their ability to form extensive intermolecular hydrogen bonds, their blending with glycerol resulted in a general increase in the macromolecules cohesion (Avena Bustillos and Krochta, 1993). Thus, the broad absorption band observed in the $3600\text{--}3000\text{ cm}^{-1}$ range can be attributed to hydrogen bonds formed between SC and glycerol hydroxyl groups (Barreto et al., 2003; Pelissari et al., 2009) as well as to the presence of unbonded N--H groups (Barreto et al., 2003; Pereda et al., 2008). As expected, the intensity of this broad band increased with the glycerol concentration since the number of available hydroxyl groups was proportionally higher. Similar comments could be applied to the asymmetric and symmetric stretching vibrations of C--H bonds at 2875 and 2925 cm^{-1} . Similar spectra were obtained for CC-based films (not shown). The intensity of the amide I band (1630 cm^{-1}) decreased when the glycerol percentage increased, as expected due to the lower proportion of protein in the final formulation. On the other hand, the band indicative of the amide II group shifted from 1510 to 1530 cm^{-1} . This effect could be associated to the existence of conformational rearrangements in the protein caused by the addition of glycerol, resulting in the decrease of inter- and intra-molecular hydrogen bonding. In addition, the intensity of these bands decreased with the increasing concentration of glycerol by the formation of --N--OH bonds, resulting in the reduction of free amine groups. Similar spectral changes were observed for the amide I band in caseinate/sorbitol films (Barreto et al., 2003). In

this sense, other bands related to the amide group (1440 and 1390 cm^{-1}) showed lower intensities when glycerol concentration increased, while, higher intensities in those bands characteristic of primary and secondary alcohols (1030 and 1100 cm^{-1}) were observed when glycerol concentration increased (Figure 4b). This trend can be qualitatively corroborated since qualitative data can be obtained by using the relationship between two peaks areas (Arrieta et al., 2012). Therefore, in order to obtain a qualitative assessment of the effect of glycerol concentration on these films, the relationship between of the areas of amide I peak (1630 nm) and the primary alcohol peak (1030 nm), was then calculated as amide I: alcohol 1° . Therefore, by comparing results of amide I: alcohol 1° ratio shown in Table 3, it could be concluded that it increased with the concentration of glycerol in both matrices, corroborating the interactions between glycerol and caseinates. Similar results were described for blends of α - and β -casein with tea polyphenols (Hasni et al., 2011). Figure 4c shows the spectra of carvacrol active films. As expected from the pure CRV spectrum (Figure 3b), formulations with this additive showed a strong wide band for O–H stretching in the $3600\text{--}3100\text{ cm}^{-1}$ region, as well as a multiband pattern in the $3100\text{--}2800\text{ cm}^{-1}$ range, overlapping with OH- and NH- stretching bands of caseinates and glycerol. However, some slight differences in a band centered at approximately 3300 cm^{-1} were noted, since its intensity was lower with the addition of carvacrol to both caseinates. This result suggests a reduction in the hydrophilic character of films. Similar results were found after the addition of tung oil to SC films (Pereda et al., 2010).

Other significant differences in FTIR spectra for films with and without CRV could be observed in the $1200\text{--}600\text{ cm}^{-1}$ region (Figure 4 d), where several peaks were detected in samples with carvacrol corresponding to phenolic bonds. Their presence gives an indication of the effective incorporation of the active additive to the biopolymer matrices.

3.3 Microstructure of edible films

The obtained films were mostly homogeneous in their surface with no apparent phase separation as evidenced from optical and SEM observations. Optical micrographs of films with CRV showed some droplets (Figure 5). The presence of these droplets can be attributed to the hydrophobicity of carvacrol that constitutes an emulsion in the caseinate-glycerol aqueous solution. However, some differences between SC and CC emulsions were observed. These differences could be explained by the relationship between α and β -caseins and the aggregation of each protein. α -casein is associated in a series of consecutive steps whereas the association of β -casein shows detergent-like micellization (Srinivasan et al., 1999). At the protein concentration level used in this work (5 wt%), both SC and CC showed preferential absorption of α -casein to the droplet surfaces. However, it can be observed that droplets in CC-CRV edible films (Figure 5d) were slightly larger than droplets in SC-CRV edible films (Figure 5b). These observations may be due to the fact that surface protein loads were higher in calcium caseinate emulsions due to the presence of large aggregates of protein (Srinivasan et al., 1999).

Figure 6 shows SEM micrographs of unplasticized CC film (Figure 6a) and plasticized with 35 wt% of glycerol (Figure 6b), both with 10 wt% CRV in their formulations. Other authors reported also homogeneous and smooth surfaces for caseinate films, particularly those with CC (Gastaldi et al., 2007) and SC/G (Fabra et al., 2009; Pereda et al., 2010). In this work no significant differences were noticed in sample surfaces by the addition of CRV, indicating a good dispersion of the antimicrobial agent in the unplasticized and plasticized matrices. Similar results were reported for coating paper based on soy protein and carvacrol (Chalier et al., 2007).

Figure 7 shows SEM micrographs taken to the cross section of unplasticized SC (Figure 7a), films plasticized with 35 wt% glycerol (Figure 7b), films plasticized SC containing CRV (Figure 7c) and unplasticized CC containing CRV (Figure 7d). In all cases, some small holes were observed due to the bubbles bursting through the surface during the casting process when water vaporization occurred (Chalier et al.,

2007). No apparent phase separation was observed in plasticized samples. This result indicates that regardless of the amount of plasticizer used in formulations, glycerol is well incorporated to the protein matrix.

3.4. Mechanical properties

Differences in tensile properties between SC and CC films with glycerol incorporated at several concentrations as well as the influence of carvacrol on their ductile behaviour were evaluated. Tables 4 and 5 show results obtained for the elastic modulus (E), tensile strength (TS) and elongation at break ($\epsilon\%$). In general terms, unplasticized films were fragile and they cracked while clamping before testing. Therefore, tensile properties were not possible to be calculated for such formulations. CC-based films showed higher E and TS values and lower $\epsilon\%$ than their SC counterparts. Therefore, SC films offer more flexible structures than CC-based materials. These results are in good agreement with Fabra et al. (2010), who claimed that the substitution of SC by CC results in an increase of stiffness and resistance to break in caseinate films.

As expected, the plasticization process caused a significant decrease in E values for all formulations. It could be observed that $\epsilon\%$ increased with the amount of glycerol, particularly for 35 wt% formulations, as expected for plasticized polymers. This parameter also increased with the addition of carvacrol for films based on SC and CC plasticized with 25 wt% of glycerol. These results demonstrated that carvacrol affect in some way the interactions between macromolecular chains in the polymer matrix, as previously indicated in the TGA study. This effect may be related to electrostatic interactions between caseinates and the active agent due to the different charge distribution into the protein chains. It can be stated that caseinates act as macroanions at the experimental pH. If considering that the pK_a of phenolic compounds such as carvacrol is around 10, the hydroxyl group should be present (Ultee et al.,

2002). These authors proposed that carvacrol could be a proton carrier by exchanging its hydroxyl proton for another cation, such as positively-charged potassium. Therefore, the exchange of the hydroxyl proton in carvacrol by mono- or dications could be the reason why CC gave more rigid structures. Other authors reported that oleic acid interactions with caseinates were reduced when calcium caseinate was added in sodium caseinate films (Fabra et al., 2010).

It is known that, in general terms, films for packaging require high flexibility at room temperature to avoid unnecessary breaking during processing and use (Martino et al, 2006). In this sense, it was demonstrated that the formulation of sodium caseinate plasticized with 35 wt% of glycerol and 10 wt% of carvacrol (SC-G35-CRV) showed the most adequate mechanical response for food contact films, with increased flexibility to ensure processing and further use while containing the antimicrobial agent to be used in active packaging formulations.

Conclusions

Transparent and homogeneous edible films based on SC, CC, SC/CRV and CC/CRV plasticized with three different glycerol concentrations were successfully obtained and characterized in terms of their structure, thermal and mechanical properties. CC edible films showed higher thermal stability than SC counterparts, due to the presence of divalent calcium cations promoting cross-linking with protein chains giving a more rigid structure, as it was also proved in tensile testing. The addition of CRV did not influence significantly the thermal stability of CC films. However, thermal stability slightly decreased for SC edible films including CRV. FTIR spectra showed that glycerol is strongly bound to caseinates, in particular when the number of hydroxyl groups increases at high glycerol concentrations. Caseinate-carvacrol interactions could suggest that the resulting materials could have more hydrophobic character than those materials without the active agent. Optical microscopy observations are in close accordance with the hydrophobic character suggested for caseinate-carvacrol

formulations, where stable emulsions are formed. Regarding mechanical properties, SC edible films showed higher flexibility than their CC counterparts. Ductile properties of films improved with the addition of glycerol, but some caution should be necessary to avoid phase separation and the consequent migration of plasticizer to foodstuff.

Therefore, it can be concluded that glycerol and carvacrol showed good compatibility with caseinates to form homogeneous films. Among all the tested formulations, the best results were found for materials with carvacrol incorporated at 10 wt% and glycerol at 35 wt %. This formulation ensures conditions for film processing as well as the significant presence of an antimicrobial additive to get an active packaging system. Consequently, these edible films show potential for their future use in fresh food preservation. Furthermore, more studies on functional properties related to food contact materials (i.e. permeability to gases, water vapour permeability, migration in different environments and antimicrobial properties) as well as the biodegradable characteristics of these formulations should be necessary and are currently on- going.

Acknowledgments

Marina Patricia Arrieta thanks Fundación MAPFRE for “Ignacio Hernando de Larramendi 2009- Medio Ambiente” fellowship (MAPFRE-IHL-01). The Spanish Ministry of Economy and Competitiveness is acknowledged by financial support (project Ref. MAT2011-28468-C02-01). Authors thank to Ferrer Alimentación S.A., for providing caseinates and to Prof. Juan López Martínez (Polytechnic University of Valencia, Spain) for his collaboration and useful discussions.

References

Abu Diak, O., Bani-Jaber, A., Amro, B., Jones, D., Andrews, G.P., (2007). The manufacture and characterization of casein films as novel tablet coatings. Food and Bioproducts Processing 85(C3), 284-290.

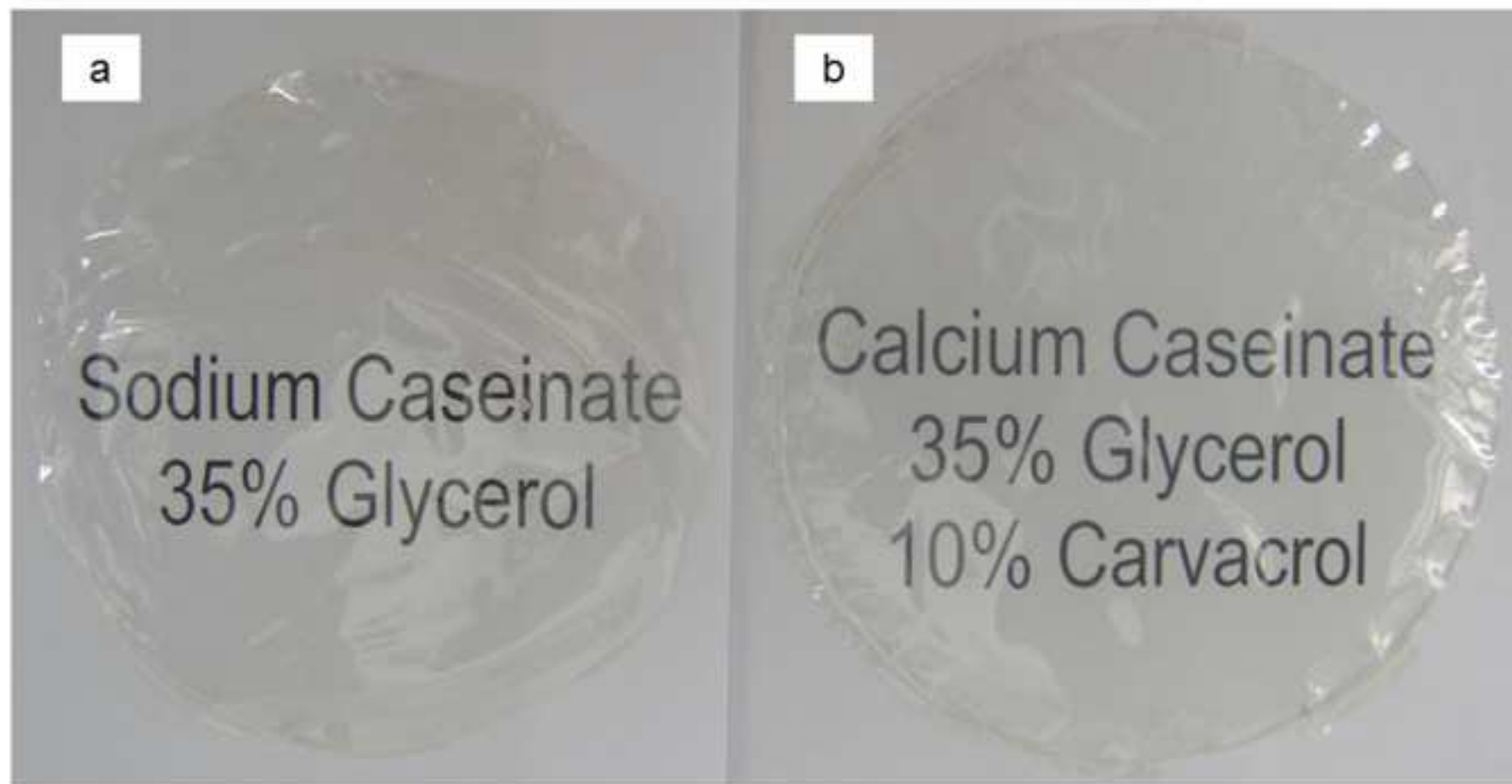
- 418 Arrieta, M.P., Parres García, F., López Martínez, J., Navarro Vidal, R., Ferrandiz, S.,
419 (2012). Pyrolysis of bioplastics waste: Obtained products from Poly(Lactic acid) (PLA).
420 DYNA 87(4), 395-399.
- 421 ASTM, (2001). Standard test method for tensile properties of thin plastic sheeting,
422 standards designation: D882-01 Annual book of ASTM standards. , Philadelphia, USA.
- 423 Audic, J.L., Chaufer, B., Daufin, G., (2003). Non-food applications of milk components
424 and dairy co-products: A review. Lait 83(6), 417-438.
- 425 Avena Bustillos, R.J., Krochta, J.M., (1993). Water vapor permeability of caseinate
426 based edible films as affected by pH, calcium cross-linking and lipid content. Journal of
427 Food Science 58(4), 904-907.
- 428 Barreto, P.L.M., Pires, A.T.N., Soldi, V., (2003). Thermal degradation of edible films
429 based on milk proteins and gelatin in inert atmosphere. Polymer Degradation and
430 Stability 79(1), 147-152.
- 431 Ben Arfa, A., Chrakabandhu, Y., Preziosi-Belloy, L., Chalier, P., Gontard, N., (2007).
432 Coating papers with soy protein isolates as inclusion matrix of carvacrol. Food
433 Research International 40(1), 22-32.
- 434 Cao-Hoang, L., Chaine, A., Gregoire, L., Wache, Y., (2010). Potential of nisin-
435 incorporated sodium caseinate films to control *Listeria* in artificially contaminated
436 cheese. Food Microbiology 27(7), 940-944.
- 437 Chalier, P., Ben Arfa, A., Preziosi-Belloy, L., Gontard, N., (2007). Carvacrol losses from
438 soy protein coated papers as a function of drying conditions. Journal of Applied
439 Polymer Science 106(1), 611-620.
- 440 Cho, S., Choi, Y., Park, S., Park, T., (2012). Carvacrol prevents diet-induced obesity by
441 modulating gene expressions involved in adipogenesis and inflammation in mice fed
442 with high-fat diet. Journal of Nutritional Biochemistry 23(2), 192-201.
- 443 Fabra, M.J., Talens, P., Chiralt, A., (2009). Microstructure and optical properties of
444 sodium caseinate films containing oleic acid-beeswax mixtures. Food Hydrocolloids
445 23(3), 676-683.

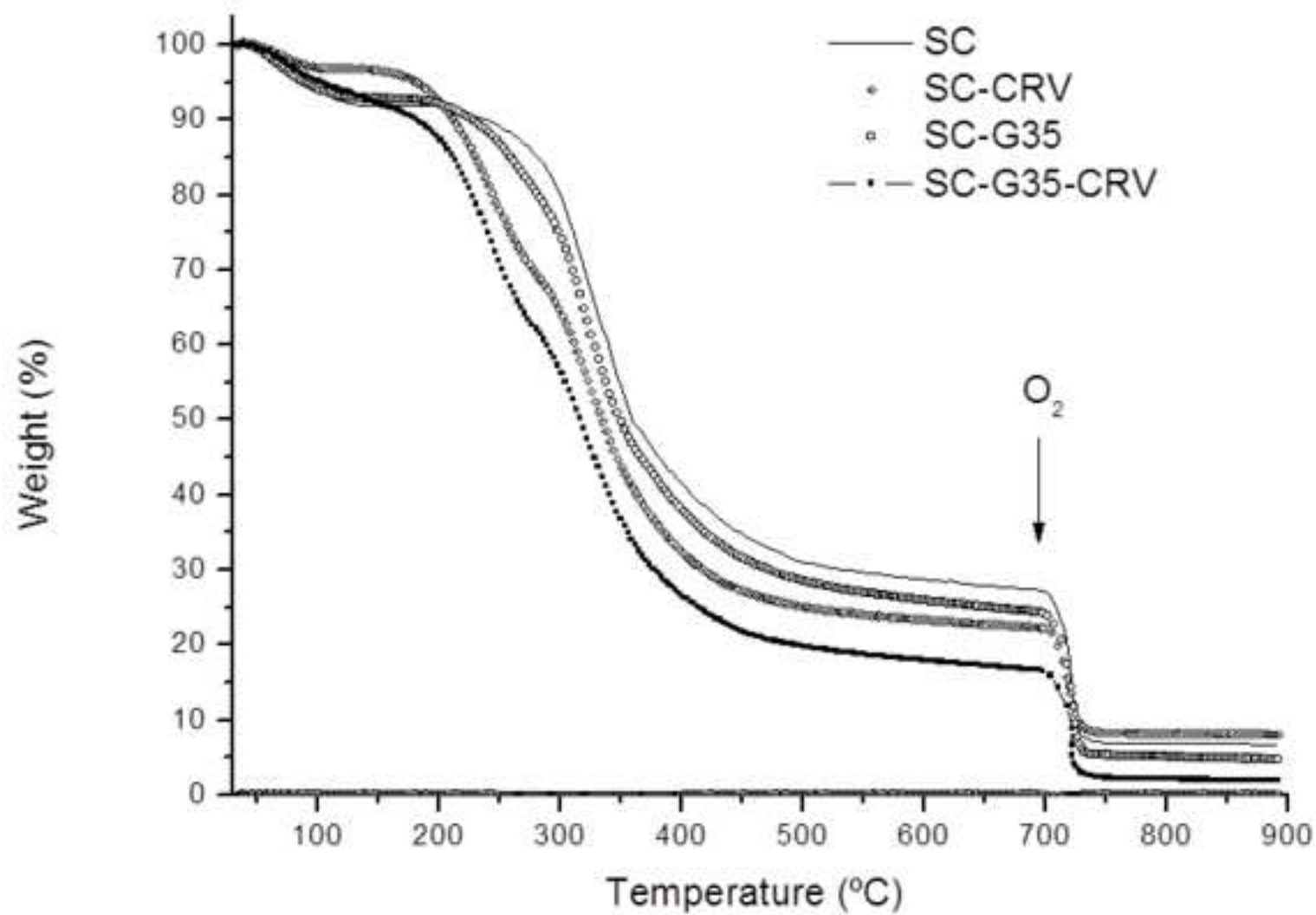
- Fabra, M.J., Talens, P., Chiralt, A., (2010). Influence of calcium on tensile, optical and water vapour permeability properties of sodium caseinate edible films. *Journal of Food Engineering* 96(3), 356-364.
- FDA Administration US
- Fernandez, C., Ausar, S.F., Badini, R.G., Castagna, L.F., Bianco, I.D., Beltramo, D.M., (2003). An FTIR spectroscopy study of the interaction between alpha(s)-casein-bound phosphoryl groups and chitosan. *International Dairy Journal* 13(11), 897-901.
- Gastaldi, E., Chalier, P., Guillemin, A., Gontard, N., (2007). Microstructure of protein-coated paper as affected by physico-chemical properties of coating solutions. *Colloids and Surfaces a-Physicochemical and Engineering Aspects* 301(1-3), 301-310.
- Gutierrez, L., Batlle, R., Sanchez, C., Nerin, C., (2010). New Approach to Study the Mechanism of Antimicrobial Protection of an Active Packaging. *Foodborne Pathogens and Disease* 7(9), 1063-1069.
- Hasni, I., Bourassa, P., Hamdani, S., Samson, G., Carpentier, R., Tajmir-Riahi, H.-A., (2011). Interaction of milk alpha- and beta-caseins with tea polyphenols. *Food Chemistry* 126(2), 630-639.
- Hernandez-Izquierdo, V.M., Krochta, J.M., (2008). Thermoplastic processing of proteins for film formation - A review. *Journal of Food Science* 73(2), R30-R39.
- Jimenez, A., Fabra, M.J., Talens, P., Chiralt, A., (2012). Effect of sodium caseinate on properties and ageing behaviour of corn starch based films. *Food Hydrocolloids* 29(2), 265-271.
- Juvonen, H., Smolander, M., Boer, H., Pere, J., Buchert, J., Peltonen, J., (2011). Film Formation and Surface Properties of Enzymatically Crosslinked Casein Films. *Journal of Applied Polymer Science* 119(4), 2205-2213.
- Kristo, E., Koutsoumanis, K.P., Biliaderis, C.G., (2008). Thermal, mechanical and water vapor barrier properties of sodium caseinate films containing antimicrobials and their inhibitory action on *Listeria monocytogenes*. *Food Hydrocolloids* 22(3), 373-386.

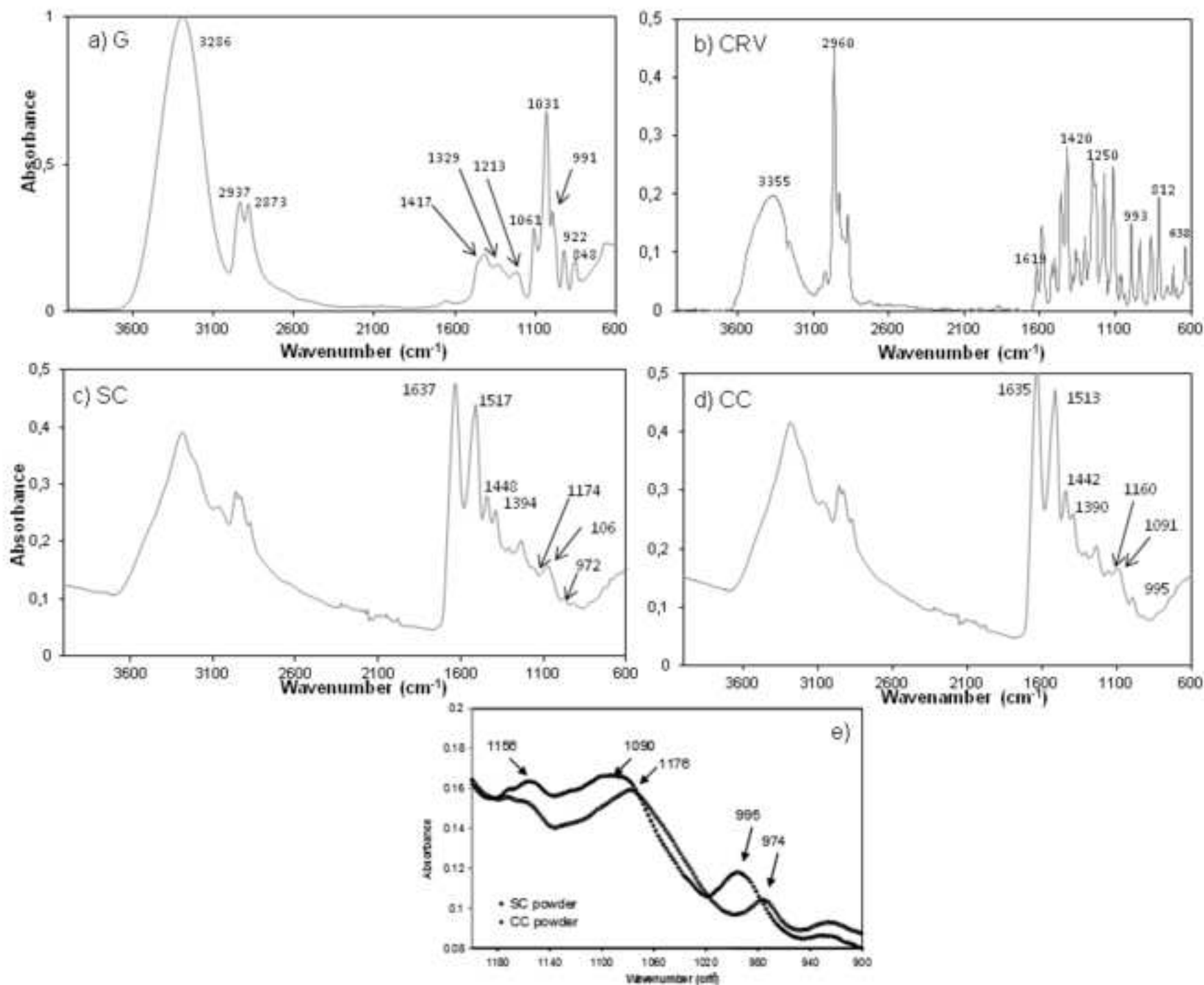
- 473 Lu, Y., Joerger, R., Wu, C., (2011). Study of the Chemical Composition and
474 Antimicrobial Activities of Ethanolic Extracts from Roots of *Scutellaria baicalensis*
475 Georgi. *Journal of Agricultural and Food Chemistry* 59(20), 10934-10942.
- 476 Martino, V.P., Ruseckaite, R.A., Jimenez, A., (2009). Ageing of poly(lactic acid) films
477 plasticized with commercial polyadipates. *Polymer International* 58(4), 437-444.
- 478 Mascheroni, E., Chalier, P., Gontard, N., Gastaldi, E., (2010). Designing of a wheat
479 gluten/montmorillonite based system as carvacrol carrier: Rheological and structural
480 properties. *Food Hydrocolloids* 24(4), 406-413.
- 481 Moreira, M.d.R., Pereda, M., Marcovich, N.E., Roura, S.I., (2011). Antimicrobial
482 Effectiveness of Bioactive Packaging Materials from Edible Chitosan and Casein
483 Polymers: Assessment on Carrot, Cheese, and Salami. *Journal of Food Science* 76(1),
484 M54-M63.
- 485 Nostro, A., Roccaro, A.S., Bisignano, G., Marino, A., Cannatelli, M.A., Pizzimenti, F.C.,
486 Cioni, P.L., Procopio, F., Blanco, A.R., (2007). Effects of oregano, carvacrol and thymol
487 on *Staphylococcus aureus* and *Staphylococcus epidermidis* biofilms. *Journal of*
488 *Medical Microbiology* 56(4), 519-523.
- 489 Oliver, C.M., Kher, A., McNaughton, D., Augustin, M.A., (2009). Use of FTIR and mass
490 spectrometry for characterization of glycated caseins. *Journal of Dairy Research* 76(1),
491 105-110.
- 492 Pelissari, F.M., Grossmann, M.V.E., Yamashita, F., Pineda, E.A.G., (2009).
493 Antimicrobial, Mechanical, and Barrier Properties of Cassava Starch-Chitosan Films
494 Incorporated with Oregano Essential Oil. *Journal of Agricultural and Food Chemistry*
495 57(16), 7499-7504.
- 496 Peltzer, M., Wagner, J., Jimenez, A., (2009). Migration study of carvacrol as a natural
497 antioxidant in high-density polyethylene for active packaging. *Food Additives and*
498 *Contaminants Part a-Chemistry Analysis Control Exposure & Risk Assessment* 26(6),
499 938-946.

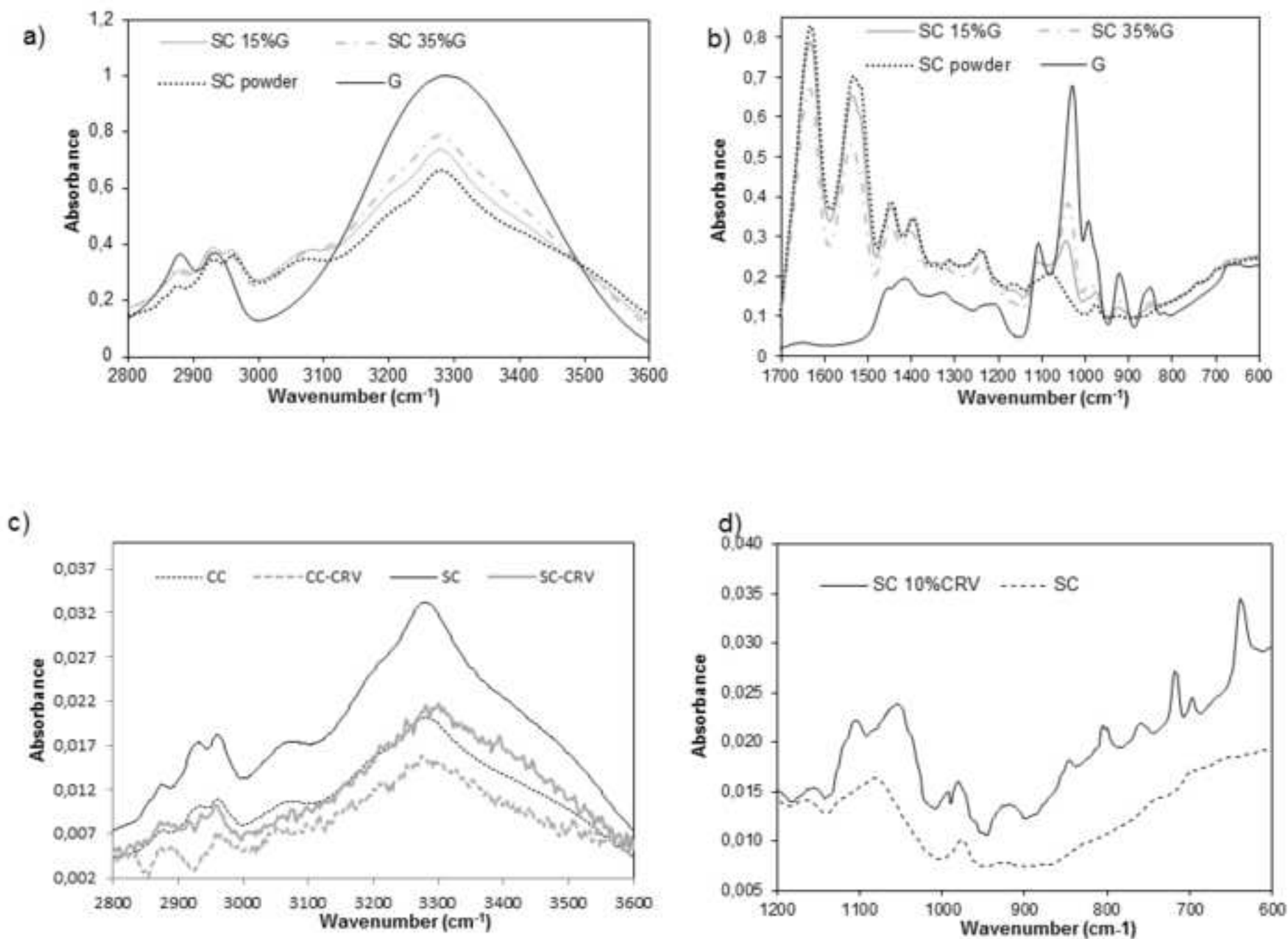
- Pereda, M., Aranguren, M.I., Marcovich, N.E., (2008). Characterization of chitosan/caseinate films. *Journal of Applied Polymer Science* 107(2), 1080-1090.
- Pereda, M., Aranguren, M.I., Marcovich, N.E., (2010). Caseinate films modified with tung oil. *Food Hydrocolloids* 24(8), 800-808.
- Pereda, M., Ponce, A.G., Marcovich, N.E., Ruseckaite, R.A., Martucci, J.F., (2011). Chitosan-gelatin composites and bi-layer films with potential antimicrobial activity. *Food Hydrocolloids* 25(5), 1372-1381.
- Persico, P., Ambroggi, V., Carfagna, C., Cerruti, P., Ferrocino, I., Mauriello, G., (2009). Nanocomposite Polymer Films Containing Carvacrol for Antimicrobial Active Packaging. *Polymer Engineering and Science* 49(7), 1447-1455.
- Pojanavaraphan, T., Magaraphan, R., Chiou, B.-S., Schiraldi, D.A., (2010). Development of Biodegradable Foamlike Materials Based on Casein and Sodium Montmorillonite Clay. *Biomacromolecules* 11(10), 2640-2646.
- Ponce, A.G., Roura, S.I., del Valle, C.E., Moreira, M.R., (2008). Antimicrobial and antioxidant activities of edible coatings enriched with natural plant extracts: In vitro and in vivo studies. *Postharvest Biology and Technology* 49(2), 294-300.
- Pretsch, E., Bühlmann, P., Affolter, C., Herrera, A., & Martínez, R. , (2001). *Determinación estructural de compuestos orgánicos.* . Springer-Verlag Ibérica., Barcelona.
- Quintavalla, S., Vicini, L., (2002). Antimicrobial food packaging in meat industry. *Meat Science* 62(3), 373-380.
- Ramos, M., Jimenez, A., Peltzer, M., Garrigos, M.C., (2012). Characterization and antimicrobial activity studies of polypropylene films with carvacrol and thymol for active packaging. *Journal of Food Engineering* 109(3), 513-519.
- Srinivasan, M., Singh, H., Munro, P.A., (1999). Adsorption behaviour of sodium and calcium caseinates in oil-in-water emulsions. *International Dairy Journal* 9(3-6), 337-341.

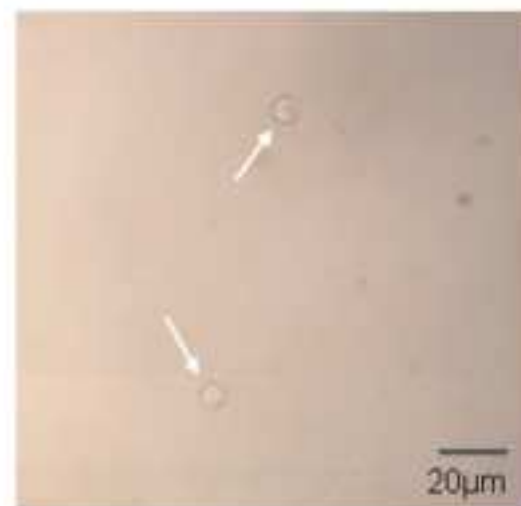
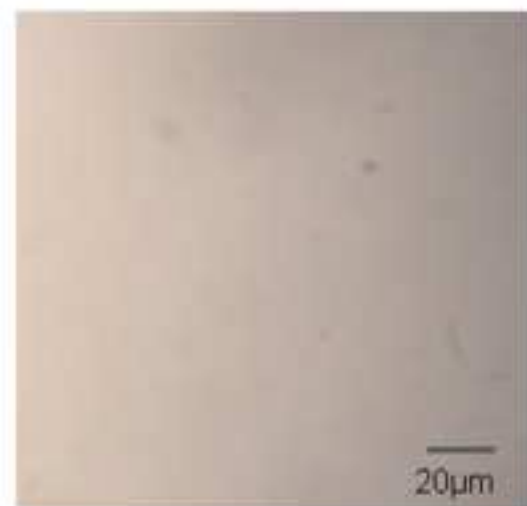
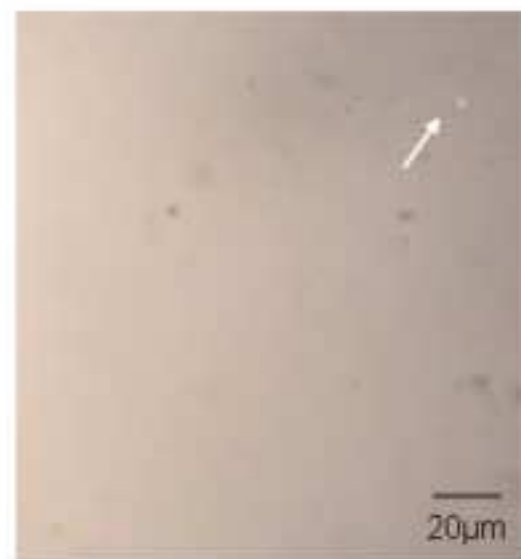
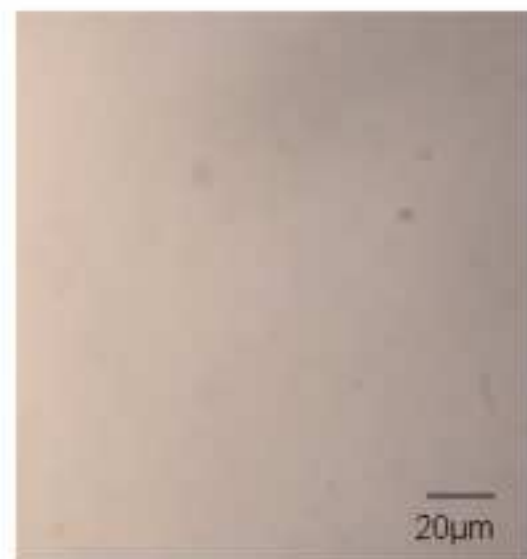
- 527 Ultee, A., Bennik, M.H.J., Moezelaar, R., (2002). The phenolic hydroxyl group of
528 carvacrol is essential for action against the food-borne pathogen *Bacillus cereus*.
529 *Applied and Environmental Microbiology* 68(4), 1561-1568.
- 530 Verbeek, C.J.R., Van den Berg, L.E., (2010). Extrusion Processing and Properties of
531 Protein-Based Thermoplastics. *Macromolecular Materials and Engineering* 295(1), 10-
532 21.
- 533 Viuda-Martos, M., El Gendy, A.E.-N.G.S., Sendra, E., Fernandez-Lopez, J., El Razik,
534 K.A.A., Omer, E.A., Perez-Alvarez, J.A., (2010). Chemical Composition and Antioxidant
535 and Anti-*Listeria* Activities of Essential Oils Obtained from Some Egyptian Plants.
536 *Journal of Agricultural and Food Chemistry* 58(16), 9063-9070.
- 537 Viuda-Martos, M., Mohamady, M.A., Fernandez-Lopez, J., Abd ElRazik, K.A., Omer,
538 E.A., Perez-Alvarez, J.A., Sendra, E., (2011). In vitro antioxidant and antibacterial
539 activities of essentials oils obtained from Egyptian aromatic plants. *Food Control*
540 22(11), 1715-1722.
- 541 Viuda-Martos, M., Ruiz-Navajas, Y., Fernandez-Lopez, J., Perez-Alvarez, J.A., (2007).
542 Antifungal activities of thyme, clove and oregano essential oils. *Journal of Food Safety*
543 27(1), 91-101.
- 544 Wang, N., Yu, J., Ma, X., Wu, Y., (2007). The influence of citric acid on the properties
545 of thermoplastic starch/linear low-density polyethylene blends. *Carbohydrate Polymers*
546 67(3), 446-453.
- 547 Ye, Z., Xiu, S., Shahbazi, A., Zhu, S., (2012). Co-liquefaction of swine manure and
548 crude glycerol to bio-oil: Model compound studies and reaction pathways. *Bioresource*
549 *Technology* 104, 783-787.

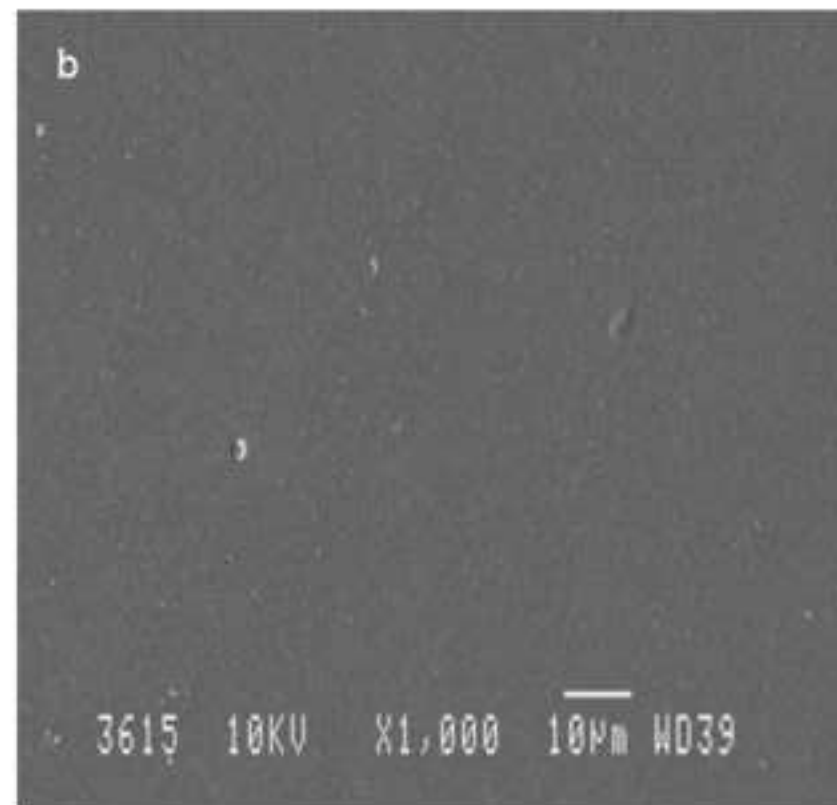
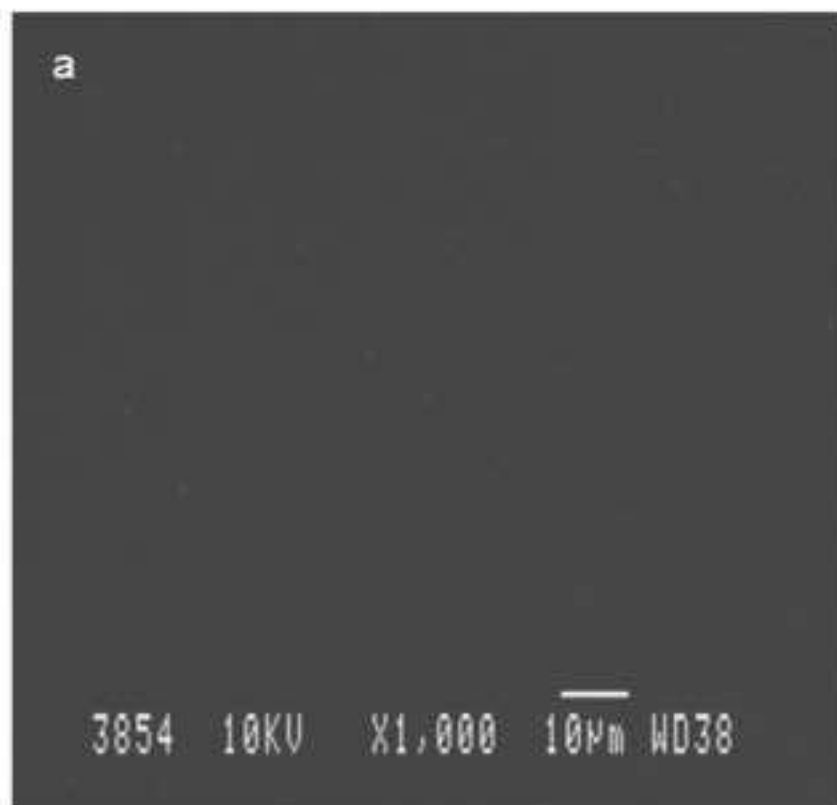


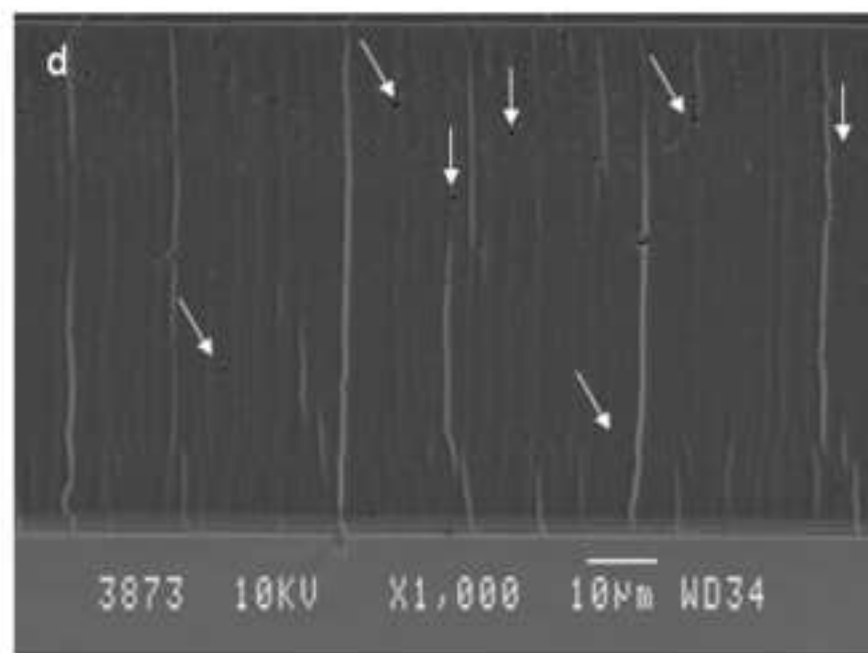
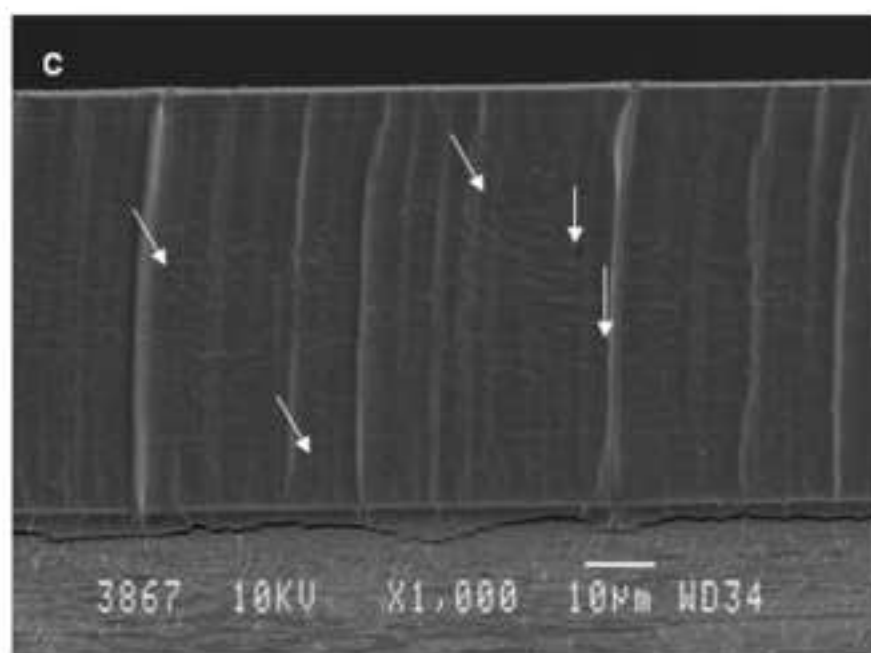
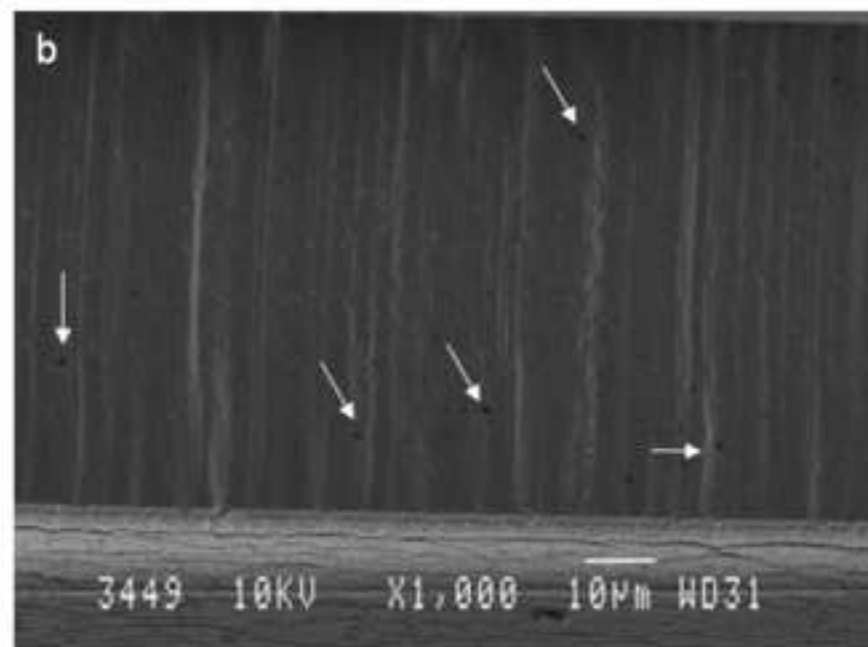
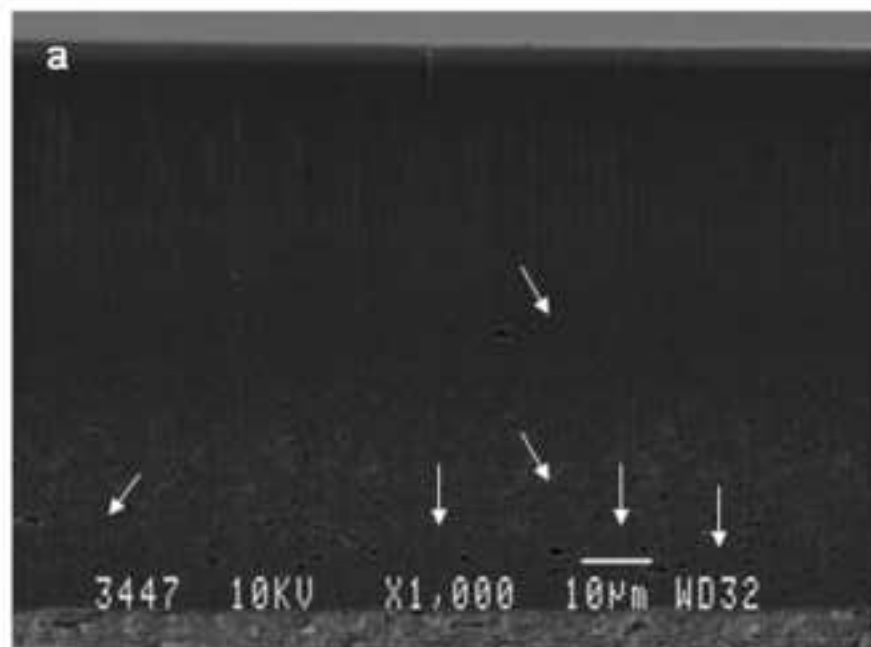












Captions to illustrations

Figure 1. Visual appearance of films based on: a) SC G35%, b) CC G35% CRV10%

Figure 2. Thermogravimetric curves of sodium caseinate (SC) edible films.

Figure 3. FTIR spectra of raw materials. a) G; b) CRV; c) SC, d) CC and d) SC + CC

Figure 4. a) and b) FTIR spectra of G, SC powered and SC edible films with two different concentration of glycerol ($3600\text{--}2800\text{ cm}^{-1}$ and $1700\text{--}600\text{ cm}^{-1}$ respectively); c) FTIR spectra of CC and SC films with and without CRV ($3600\text{--}2800\text{ cm}^{-1}$) and d) FTIR spectra of SC films with and without CRV ($1200\text{--}600\text{ cm}^{-1}$).

Figure 5. Optical micrograph (50x) of edible films surface: a) SC G35%, b) SC G35% CRV10%, c) CC G35% and d) CC G35% CRV10%.

Figure 6. SEM micrographs (1000x) of edible films surface: a) CC pure and b) CC G35% CRV10%.

Figure 7. SEM micrograph (1000x) of SC films cross section: a) SC unplasticized, b) SC G35%, c) SC G25% CRV10% and d) CC CRV10%

Table 1. Thermal parameters of SC samples obtained from TGA

Samples	Thermogravimetric parameters					
SC:G:CRV	T ₀ (°C)	Stage I		Stage II	Stage III	Residue at 900 °C (%)
		Interval (°C)	T _{max I} (°C)	T _{max II} (°C)	T _{max III} (°C)	
1:0:0	241	30-164	78	-	326	6.7
1:0.15:0	238	30-142	78	223	322	7.0
1:0.25:0	217	30-128	84	249	320	5.5
1:0.35:0	205	30-128	69	244	326	3.7
1:0:0.10	226	30-140	81	-	320	4.8
1:0.15:0.10	202	30-131	81	232	322	5.0
1:0.25:0.10	200	30-121	69	243	320	3.8
1:0.35:0.10	180	30-104	69	243	320	1.9

Table 2. Thermal parameters of CC samples obtained from TGA

Samples		Thermogravimetric parameters				Residue at 900 °C (%)
CC:G:CRV	T ₀ (°C)	Stage I		Stage II	Stage III	
		Interval (°C)	T _{max I} (°C)	T _{max II} (°C)	T _{max III} (°C)	
1:0:0	220	30-160	81	-	338	6.0
1:0.15:0	214	30-154	101	235	332	5.3
1:0.25:0	207	30-126	83	232	330	5.0
1:0.35:0	193	30-116	70	220	331	5.2
1:0:0.10	223	30-152	76	-	335	5.0
1:0.15:0.10	211	30-161	107	258	328	5.3
1:0.25:0.10	202	30-152	93	261	335	4.2
1:0.35:0.10	199	30-111	76	262	335	3.1

Table 3. Comparison between FTIR amide (1630 nm) and alcohol (1030 nm) bands of SC and CC samples

SC:G:CRV						
	1:0.15:0	1:0.25:0	1:0.35:0	1:0.15:0.10	1:0.25:0.10	1:0.35:0.10
Amide I : alcohol 1°	1:0.23	1:0.36	1:0.49	1:0.54	1:0.61	1:0.83
CC:G:CRV						
	1:0.15:0	1:0.25:0	1:0.35:0	1:0.15:0.10	1:0.25:0.10	1:0.35:0.10
Amide I : alcohol 1°	1:0.36	1:0.71	1:0.84	1:2.02	1:2.13	1:2.17

Table 4. Tensile properties of SC edible films ($n=5$)

SC:G:CRV	Tensile properties		
	ϵ_B (%)	E (MPa)	TS (MPa)
1:0.15:0	17 ± 6	178 ± 80	1.50 ± 0.20
1:0.25:0	32 ± 1	31 ± 10	0.62 ± 0.19
1:0.35:0	79 ± 11	7 ± 1	0.14 ± 0.06
1:0.15:0.10	27 ± 5	82 ± 15	0.73 ± 0.08
1:0.25:0.10	81 ± 3	29 ± 8	0.42 ± 0.15
1:0.35:0.10	62 ± 11	8 ± 2	0.09 ± 0.02

Table 5. Tensile properties of CC edible films ($n=5$)

CC:G:CRV	Tensile properties		
	ϵ_B (%)	E (MPa)	TS (MPa)
1:0.15:0	6 ± 2	424 ± 15	1.78 ± 0.09
1:0.25:0	9 ± 2	272 ± 6	0.54 ± 0.01
1:0.35:0	36 ± 2	39 ± 3	0.50 ± 0.02
1:0.15:0.10	5 ± 2	137 ± 2	3.02 ± 0.04
1:0.25:0.10	20 ± 3	61 ± 7	1.20 ± 0.05
1:0.35:0.10	33 ± 8	36 ± 6	0.26 ± 0.03

- Transparent and homogeneous edible active films based on caseinates were obtained.
- Sodium Caseinate films showed higher flexibility than the Calcium Caseinate ones.
- Glycerol and carvacrol showed good compatibility with caseinates to form films.